Fusion Engineering and Design 124 (2017) 77–81

Fusion Engineering and Design

journal homepage: www.elsevier.com/locate/fusengdes

Mechanical pre-dimensioning and pre-optimization of the tokamaks' toroidal coils featuring the winding pack layout

Anatoly Panin[a,*], Wolfgang Biel[a], Philippe Mertens[a], Francois Nunio[b], Louis Zani[c]

[a] Forschungszentrum Jülich GmbH, Institut für Energie und Klimaforschung—Plasmaphysik, Partner of the Trilateral Euregio Cluster (TEC), 52425 Jülich, Germany
[b] Commissariat à l'Energie Atomique et aux Energies Alternatives, CEA Saclay IRFU/SIS, 91191 Gif-sur-Yvette, France
[c] Commissariat à l'Energie Atomique et aux Energies Alternatives, CEA Cadarache IRFM/STEP, 13108 St-Paul Lez Durance, France

HIGHLIGHTS

- Structural integrity of superconducting magnets that are key elements of a fusion reactor is to be ensured.
- A calculation procedure that estimates mechanical strength of tokamak TFCs and features its pre-optimization is described.
- The procedure has been benchmarked and used for pre-dimensioning and pre-optimization of the 2015 DEMO TFC layout.
- Compared to time consuming 3D analysis the procedure immediately spots TFC strength issues and optimize layered windings.
- After coil winding pre-optimization the minimum coil radial built that is a key design parameter is defined.

ARTICLE INFO

Article history:
Received 29 September 2016
Received in revised form 7 February 2017
Accepted 18 April 2017
Available online 29 April 2017

Keywords:
Fusion magnets
Electromagnetic loads
Winding pack
Structural analysis
Coils pre-dimensioning

ABSTRACT

The structural integrity of superconducting magnets that are key elements of a fusion reactor must be ensured. At an early design stage relatively simple calculation tools can greatly facilitate design optimization. The main objective of this paper is the mechanical pre-dimensioning of the tokamak toroidal field coils by simple means prior to the global 3D numerical modeling. A semi-analytical calculation tool that reasonably estimates the static strength of the toroidal field coil under the electromagnetic forces at the critical location (inner leg equatorial plane) is described. The novelty of the approach is that it treats not only the massive coil casing but also the winding pack conductor jacket under an essentially 3D stress state. The calculation tool features pre-optimization of the coil winding for graded layered winding layouts. The minimum space (radial built) required for the coil inboard portion that is a key design parameter is defined after possible winding pre-optimization. The procedure has been successfully benchmarked against numerical solutions and has been used for pre-dimensioning the toroidal coils in the frame of the current 2015 DEMO activity.

1. Introduction

Successful operation of Demonstration Reactors is a key step in fusion development. High magnetic fields produced by the superconducting magnets are crucial for optimization of the performance of such a fusion reactor. The main structural issues of the toroidal field coil (TFC) system are briefly overviewed in Chapter 2.

Combinations of calculation approaches, reasonable modeling simplifications and clever prioritization at each analysis phase facilitate design optimization by relatively simple and "inexpensive" calculation tools [1]. A simple procedure for TFC mechanical pre-dimensioning that has been proved to be very useful and time saving at an early design stage is described in Chapter 3. The approach novelty is that it deals not only with the static strength of the coil casing at the coil inboard (e.g. [2]) but also treats in detail the winding pack wound with the cabled conductor. The tool features pre-optimization of the layered windings by grading conductors with respect to their radial and toroidal walls separately. The minimum space (radial built) for the coil inboard portion required to satisfy static strength criteria is defined. The procedure was successfully benchmarked against the FE solutions and used for pre-dimensioning the toroidal coils for the ongoing 2015 European DEMO project.

---

* Corresponding author.
E-mail address: a.panin@fz-juelich.de (A. Panin).

http://dx.doi.org/10.1016/j.fusengdes.2017.04.065

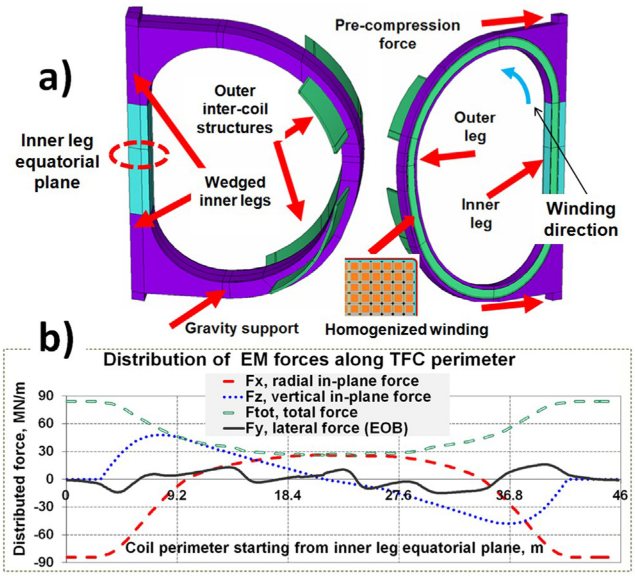

Fig. 1. Example of TF coil structure.

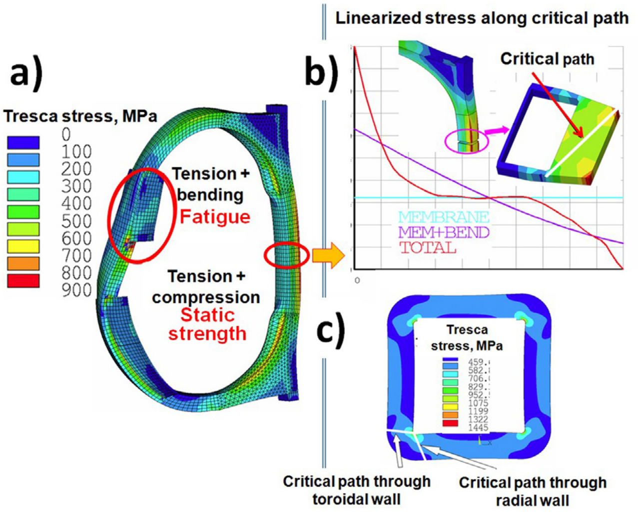

Fig. 2. Tresca stress in TF coil due to EM loading.

2. TF coil system structural issues

Typical TFC system (Fig. 1a) comprises a number of coils arranged symmetrically around the torus axis. At the inboard the coils are wedged to support the centripetal Lorentz forces due to the TFC energizing. These in-plane forces (Fig. 1b) acting normal to the winding centerline cause significant toroidal compression in the wedged coils' portions and expand the coil both radially and vertically. With regard to the in-plane loading the most critical coil region is at the equatorial plane of the inner leg where the huge wedge compression is coupled with the vertical tension (Fig. 2a). The matter is usually aggravated by a lack of space for supporting structures. At the outboard the coils are connected via the outer intercoil structures that sustain coils cyclic tilting due to the out-of-plane forces that are caused by interaction of the TFCs currents with magnetic fields of the central solenoid, poloidal coils and plasma. The coils' lateral deflection and fatigue are the issues at coil outboard. Strength of the coil case and conductors under combined loading is of concern (Fig. 2).

3. TFC under in-plane loading: pre-dimensioning and pre-optimization

3.1. Electromagnetic estimations for TF coils

A typical TFC cross-section is shown in Fig. 3a. The TF coil can be considered like a set of conducting shells [3]. The magnetic field at the conductor due to the coils' currents at the coil inboard reaches:

$$B^{max} = \mu_0 N_{coil} I_{coil} / (2\pi R_{in}) \qquad (1)$$

where: $\mu_0 = 4\pi \times 10^{-7}\,\mathrm{H\,m^{-1}}$, N_{coil} – number of coils, I_{coil} –coil current. The maximum distributed pressure force in the winding and the maximum cumulated pressure from the winding acting on the coil case are expressed as:

$$F_{EM} = 1/2B^{max} I_{coil} \text{ and } P_{EM}^{WP} = F_{EM}/H_{WP} \qquad (2)$$

for P_{EM}^{WP},H_{WP} see Fig. 3. The vertical force acting on the coil half at its equatorial plane is calculated:

$$F_z^{coil} = \pi \left(B^{max}\right)^2 R_{in}^2 \ln\left(\frac{R_{out}}{R_{in}}\right) \frac{1}{\mu_0 N_{coil}} \qquad (3)$$

The vertical force taken by the coil inner leg can be assumed as $F_z^{inner} \approx 1/2F_z^{coil}$. The force share between the coil case F_z^{SS} and the winding F_z^{WP} can be calculated from F_z^{inner} in proportion to their stiffness when no the coil case/WP poloidal sliding is assumed.

3.2. TFC stress-state: equatorial plane of inner leg

The massive coil case can be considered as a ring under the uniform external pressure P_0 coming from the WP (Fig. 4b). This pressure causes significant wedge compression σ_{fi}^{case}. The case vertical stress is determined by the EM vertical force on the case and is defined as $\sigma_z^{SS} = F_z^{SS}/A_{SS}$ where A_{SS} is the case area.

The WP is considered as a bulk homogenized structure having the orthotropic properties [4]. Loaded by the volumetric EM forces it presses on the ring (case) and follows its inward movement. This inward movement of the wedged coils results in the winding lateral compression σ_y^{WP} (Fig. 4). The vertical stress in the WP is determined by the vertical electromagnetic force taken by the winding and is defined as $\sigma_z^{WP} = F_z^{WP}/A_{WP}$where A_{WP} is the winding area.

If we call $P_{EM} = F_{EM}/2R_2\alpha$ and $k = 2F_{pull}/F_{EM}$, than uniform pressure on the ring accounting for F_{pull} is:

$$P_0 = \frac{F_{EM} - 2F_{pull}}{2R_2\alpha} = P_{EM}(1-k) \qquad (4)$$

The ring inward movement under the external pressure coming from the winding (not accounting for F_{pull}) in assumption of the generalized plane strain condition is:

$$u_x^{EM} = -P_{EM}\frac{R_2}{E^{SS}}\left(\frac{R_2^2 + R_1^2}{R_2^2 - R_1^2} - \nu_{SS}\right) \qquad (5)$$

E^{SS},ν^{SS}- steel Young's modulus and Poisson's ratio.

The ring inward movement under P_0 with the account for its toroidal contraction due to F_z^{SS} can be written:

$$u_x^{WP} = u_x^{case} = u_x^{EM}(1-k) + u_x^Z \qquad (6)$$

where: $u_x^Z = -\nu_{SS}\frac{\sigma_z^{SS}}{E^{SS}}R_2, \sigma_z^{SS} = F_z^{SS}/A_{SS}, A_{SS}$- case area. Denoting $C_1 = 2\tan(\alpha)/H_{WP}$, the winding lateral compressive strain due to WP radial movement is written:

$$\varepsilon_y^{WP} = u_x^{WP} C_1 = -\nu_{xy}\frac{\sigma_x^{WP}}{E_x^{WP}} + \frac{\sigma_y^{WP}}{E_y^{WP}} - \nu_{yz}^{WP}\frac{\sigma_z^{WP}}{E_y^{WP}} \qquad (7)$$

where: σ_x^{WP} is the x component of the winding radial stress due to the volumetric EM loading, $\sigma_z^{WP} = F_z^{WP}/A_{WP}$ and A_{WP} is the wind-

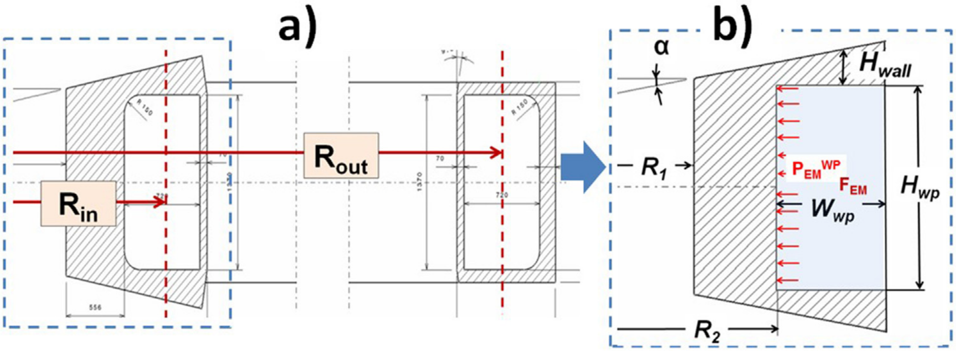

Fig. 3. Typical TFC cross-section at coil equatorial plane (left) and sketch of the simplified inner leg cross-section (right).

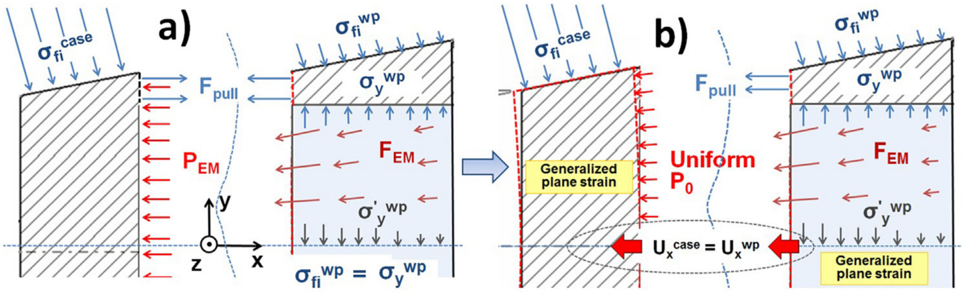

Fig. 4. Sketch of model problem.

ing area. If we denote: $\varepsilon'{}_y = \nu_{xy}\sigma_x^{WP}/E_x^{WP}$, and $C_2 = E_y^{WP}$ (winding Young's modulus) then:

$$\sigma_y^{WP} = \left(\varepsilon_y^{WP} + \varepsilon'{}_y + \varepsilon'{}_y\right) E_y^{WP} = \\ = \left\{C_1\left[u_x^{EM}(1-k) + u_x^z\right] + \varepsilon'{}_y + \varepsilon'{}_y\right\} C_2 \tag{8}$$

On the other hand

$$\sigma_y^{WP} = \frac{F_{pull}}{W_{WP}\tan\alpha} = kP_{EM}/C_3 \tag{9}$$

where: $C_3 = \frac{W_{WP}\tan\alpha}{R_2\alpha}$

If we equate the expressions (1) and (2) then:

$$k = \frac{\left[C_1\left(u_x^{EM} + u_x^z\right) + \varepsilon'{}_y + \varepsilon'{}_y\right] C_2C_3}{P_{EM} + C_1 u_x^{EM}\cdot C_2C_3} \tag{10}$$

Having the parameter k defined, one can calculate the coil (and WP) inward movement $u_x^{case} = u_x^{WP}$, the case hoop stress σ_{fi}^{case} and the lateral compression in WP σ_y^{WP}. The radial stress in the WP σ_x can be assumed to increase linearly from zero at the plasma side to P_{EM}^{WP} at the winding outside. To account for a distribution of σx and for a change of E_y^{WP} through the winding (graded layered WPs) more general form of the expression (10) is written:

$$k = \sum_{i=1}^{Ngrade}\left[C_1\left(u_x^{EM} + u_x^z\right) + \varepsilon'{}_y(i) + \varepsilon'{}_y(i)\right]\cdot \\ \cdot\frac{C_2(i)C_3(i)}{P_{EM} + C_1u_x^{EM}\cdot\sum_{i=1}^{Ngrade} C_2(i)C_3(i)} \tag{11}$$

Thus, all important stress components in the coil case (hoop and vertical stresses – the radial one can be neglected) and in the homogenized WP (radial, lateral and vertical ones) are available for the strength estimations.

3.3. Main results of benchmarking

Fig. 5 shows results of benchmarking of the main stress components in the homogenized winding calculated with the semi-analytical tool against 3D FE calculations. For the 2014 DEMO layout a very good agreement was found (Fig. 5a). For the 2015 layout the lateral stresses in the winding calculated with the tool turned out to be higher than those given by FE analysis (Fig. 5b). The matter is that for this layout the coils' wedging is not engaged all over the WP width (Fig. 5c) and the winding is less compressed at the plasma side. This feature is planned to be implemented in the tool.

3.4. Winding stresses: from global to local

The calculated hoop compression and vertical tension in the coil case can be reasonably considered as the maximum and minimum principal stresses. This makes it possible to directly construct the equivalent Tresca stress to be compared with the allowable primary membrane stress for the case structural steel [5]. For the homogenized winding the calculated stresses need to be recalculated to the conductor walls which mostly take the radial and lateral compression that is coupled with the conductor vertical tension. The procedure looks like:

- The radial stress that is assumed to increase linearly through the WP is calculated for each WP grade and recalculated to the conductor radial walls.
- The lateral stress is calculated for each WP grade and recalculated to the conductor toroidal walls.
- To construct the Tresca stress the compressive stresses in the conductor walls are coupled with the vertical tensile stress that is calculated for each WP grade and recalculated to the conductor walls.
- For each conductor grade the calculated Tresca stress in the conductor walls is checked against the allowable primary membrane stress [5].

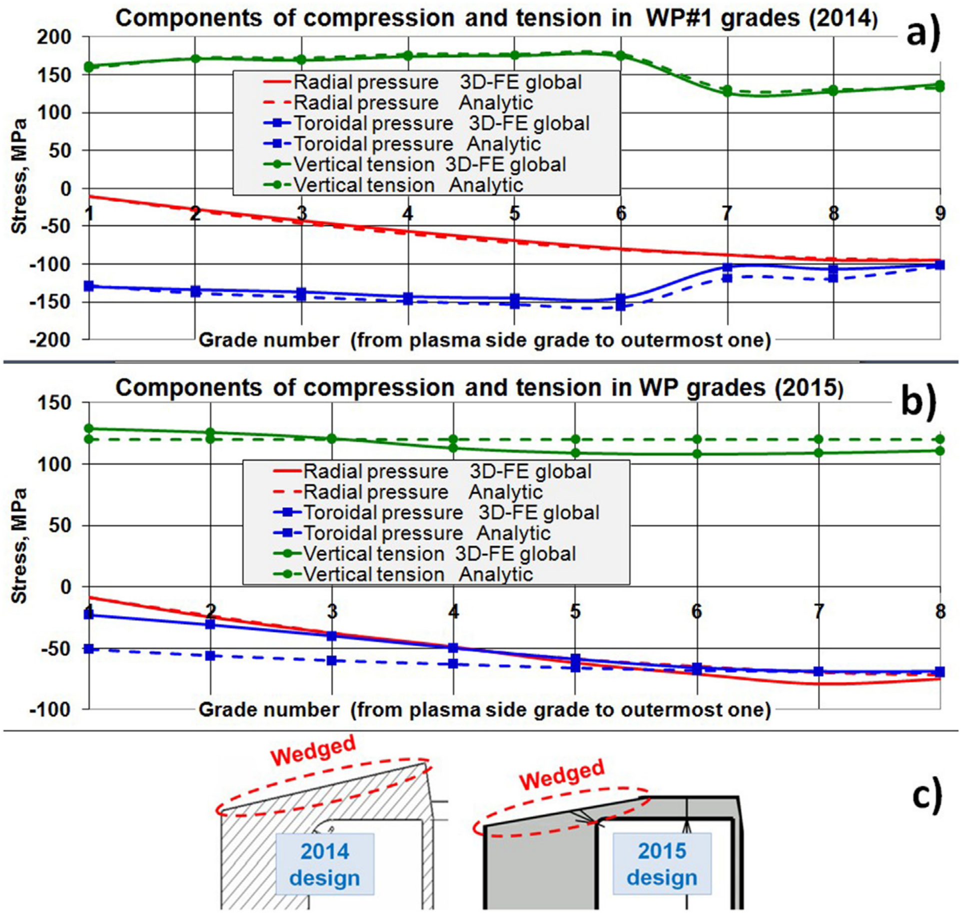

Fig. 5. Distribution of important stress components over homogenized WP grades (2014 & 2015 DEMO TFC layouts).

Table 1
Linearized Tresca stress over conductor jacket walls vs. allowable stress (2014 TFC design, WP#2 option).

	Radial wall	Toroidal wall	Allowable stress
Membrane, MPa	669	648	667

Critical locations were found (pre-dimensioning tool) for the 2014 WP layout where the conductor stresses exceed limits. This agrees with the results of the TFC 3D FE modeling [1] represented in Table 1.

3.5. *Winding pre-optimization and TFC pre-dimensioning*

- The winding smeared properties and then the important stress components are calculated for the coil case and for the initial layout of the winding.
- Tresca stress is constructed for the coil case and for the WP conductor walls (all grades), and compared with the allowable primary membrane stress.
- If the strength limits in the conductor walls are not met the mechanical optimization starts by grading the radial and toroidal conductor walls separately.
- By redistributing available “structural steel” the thickness of the radial conductor walls is modified to satisfy the strength criteria for these walls in each conductor grade. The “left structural steel” is redistributed between the conductor toroidal walls.
- The new orthotropic winding properties are calculated. The changed WP toroidal stiffness results in a change of the WP toroidal compression that, in turn, impacts on the case/WP radial movement.
- Basing on the recalculated stresses the available structural steel is further redistributed between the toroidal conductor walls to satisfy the strength criteria for these walls. Several iterations are usually needed (each requires recalculation of the winding properties) to converge. Note that the “mechanically pre-optimized” design may not be feasible from a manufacturing/assembly viewpoint and serves only as the first step for further WP optimization.

There are two optimization options available:

1. The space allocated for the superconducting cable is kept unchanged. This possibly results in a not fully mechanically optimized winding layout
2. The full mechanical optimization is performed on the expense of the space for the superconducting cable.

The conductor stresses calculated for the 2015 WP layout prior to 3D FE analysis proved to violate the conductor stress limits. More space for the coil structures was requested. For the modified layout the FE analysis revealed no membrane stresses in the conductor violating criteria as it was predicted while the conductors must be further optimized regarding their wall bending (Table 2).

4. Conclusions

TFC pre-dimensioning and pre-optimization at an early design stage was proved to be extremely effective. A calculation tool that reasonably estimates the coil mechanical strength under the dom-

Table 2
Linearized Tresca stress over conductor jacket walls vs. allowable stresses (2015 TFC design).

	Radial wall	Toroidal wall	Allowable stress
Membrane, MPa	591	583	667
Membrane + bending, MPa	891	858	867

inating EM loading has been developed, benchmarked and used for the coil pre-dimensioning and pre-optimization in the frame of the ongoing 2015 DEMO activity.

The approach novelty is that it treats the winding pack conductor in detail under 3D stress-strain state. This makes possible an effective pre-optimization of the layered windings by grading conductors in regard to their radial and toroidal walls separately. After the winding is mechanically pre-optimized the requirements for the minimum coil space at its inboard portion are defined.

Acknowledgments

This work has been carried out within the framework of the EUROfusion Consortium and has received funding from the Euratom research and training programme 2014–2018 under grant agreement No 633053. The views and opinions expressed herein do not necessarily reflect those of the European Commission.

References

[1] A. Panin, et al., Approaches to analyze structural issues of the European DEMO Toroidal Field Coil System at an early design stage, IEEE Trans. Appl. Superconduct. 26 (4) (2016), http://dx.doi.org/10.1109/TASC.2016.2516998.
[2] J.-L. Duchateau, et al., Conceptual integrated approach for the magnet system of a tokamak reactor, Fusion Eng. Des. 89 (2014) 2606–2620, http://dx.doi.org/10.1016/j.fusengdes.2014.06.012.
[3] R.J. Thome, J.M. Tarrh, MHD and Fusion Magnets, Field and Force Design Concepts, John Wiley & Sons, 1982.
[4] A.I. Borovkov, et al., FE analysis of effective mechanical and thermal characteristics of micro heterogeneous toroidal field coils, IEEE Trans. Magn. 28 (1992) 927–930.
[5] ITER Magnet Structural Design Criteria, Part 1: Main Structural Components and Welds (ITER_D_2FMHHS), Part 2: Magnet Windings (ITER_D_2ES43 V), 2012.